Collective global dynamics in Au+Au collisions at the BNL AGS

L. Bravina,[1] L.P. Csernai,[1] P. Lévai,[1,2] and D. Strottman[1,3]
[1] *Physics Department, University of Bergen, 5007 Bergen, Norway*
[2] *KFKI Research Institute for Particle and Nuclear Physics, 1525 Budapest, Hungary*
[3] *Theoretical Division, Los Alamos National Laboratory, Los Alamos, New Mexico 87545*
(Received 15 March 1994)

Signatures of collective effects are studied in the quark gluon string model and in the fluid dynamical model for Au+Au collisions at 11.6A GeV/c. In the fluid dynamical model the dependence of observables on the quark-gluon plamsa (QGP) formation in the equation of state is pointed out although the maximal total amount of pure QGP formed is only about 8 fm^3 in these reactions. In contrast to the baryon rapidity distribution, the in-plane transverse flow and especially the squeeze-out effect are particularly sensitive to the EOS. In the QGSM the lifetime and extent of baryon density in strings are studied. The QGSM picture is very similar to the one obtained in the fluid dynamical model with a pure hadronic EOS.

PACS number(s): 24.85.+p, 25.75.+r, 13.85.−t, 21.65.+f

I. INTRODUCTION

In most reaction models of relativistic heavy ion collisions where a first-order phase transition to the quark-gluon plasma (QGP) is considered, it is assumed that the phase transition is rapid compared to the dynamics of compression or expansion, and consequently instantaneous phase equilibrium is assumed to be present. This assumption leads to a mixed phase according to the Maxwell construction, which decreases the pressure in a large domain of the phase space even if only a small amount of QGP is present. Thus even a small impurity of QGP in the matter can lead to a significant change of the equation of state (EOS). Recent explicit calculations of QGP-hadronic matter transition in the framework of homogeneous nucleation theory [1, 2] indicate that the dynamical hadronization picture is not far from the idealized Maxwell scenario. This assumption is generally used in three-dimensional fluid dynamical models where the phase transition to a QGP is taken into account [3–7].

In string models QGP formation is not considered directly, but intermediate nonhadronic objects, strings, are formed. These absorb an essential part of energy and baryon charge during the initial stages of the reaction. As pointed out earlier [3], the string density may become very large, so that string-string interactions in principle should not be neglected. Comparison of string model predictions with experiments indicates that an accurate description of massive strange baryons is possible only if string-string fusion, string-rope formation, or di-string formation are considered. The formation of such large nonhadronic objects is necessary to provide sufficient energy for massive baryon formation. The dense soup of interacting and partly fused strings can be considered as a nonequilibrated precursor of the quark-gluon plasma. The actual EOS of such string models has not been evaluated so far.

In the present work fluid dynamical model calculations are presented and discussed for AGS reactions. The validity of the results is analyzed by comparing them to quark gluon string model (QGSM)[3] calculations, where most of the assumptions of perfect fluid dynamics are not present. The Monte Carlo version of the QGSM describes experimental data [8] quite well [5], and it has been used as a tool to study detailed microscopic processes. The fluid dynamical model, on the other hand, enables us to determine which observable quantities are the most sensitive to the underlying EOS in the collision.

II. COLLECTIVE REACTION DYNAMICS

Let us first demonstrate the flow patterns in central reactions for Au+Au at 11.6A GeV/c in the fluid dynamical model with two equations of state, one with pure hadronic matter and the other including a strong first-order phase transition to QGP [3]. If a QGP is present in the EOS the fluid dynamical model predicts the formation of a region containing pure QGP. The maximum center-of-mass volume of pure QGP produced in central collisions is only 8 fm^3, i.e., about 1% of the total Lorentz contracted precollision volume of the system. This can be compared to 50 fm^3 in Pb+Pb reactions at 160A GeV, which is one-fourth of the initial volume of the system. Thus the amount of QGP at AGS energies is unlikely to be sufficient to provide any direct QCD signal like J/Ψ suppression or in di-lepton emission. However, as we will see, the secondary changes due to the softness of the QGP EOS may still be detectable.

The average baryon density increases to 10 (7) n_0 (where n_0 is the normal nuclear density) during a central Au+Au collision with a QGP (hadronic) EOS. The central baryon density is 14 (9) n_0 in the same collision, while with increasing impact parameter, $b/b_{\max}$, the central density decreases and above $b/b_{\max} = 0.5$ the central density does not depend on the EOS, i.e., the effect of a QGP is not manifested in peripheral collisions ($b_{\max} = 2R_{\mathrm{Au}} = 2 \times 6.7$ fm). In central collisions the break-up time is around 10–12 (7–8) fm/c, respectively,

for the two EOS's, *i.e.*, the phase transition leads to an increase of the collision time by about 30–40% (see Fig. 1). The time is measured in the center-of-mass frame from the moment of the impact.

In the QGSM the baryon density has a behavior very similar to that observed in the fluid dynamical model with a pure hadronic equation of state: the maximum central (average) baryon density is about 10 (4) n_0 for central and around 2 (1.1) n_0 for the peripheral Au+Au collisions. (Fig. 2). The dense baryonic matter disintegrates in 9–10 fm/c after the first collision. In the QGSM the local rest baryon density, n_B, was calculated as a sum of baryon charge numbers, q_i^b, in the cell, $\mathsf{N}_b^{\rm cell} = \sum_{i\in{\rm cell}} q_i^b$, divided by the volume of the cell in the Eckart local rest frame, $n_B = \mathsf{N}_b^{\rm cell}/(\gamma_{\rm cell}\mathsf{V}_{\rm cell})$, where $\gamma_{\rm cell}$ is expressed via the particle four-flow, $N^\nu(x)$, of the classical gas: $\gamma_{\rm cell} = u^0 = N_b^0/(N_b^\nu N_{b\nu})^{1/2}$, and $N_b^\mu = \int \frac{d^3p}{p^0} p^\mu \sum_b q^b\, f_b(x,p) = \sum_{i\in{\rm cell}} q_i^b\, p_i^\mu/p_i^0$.

The average density was calculated in a rectangular grid of $\Delta x\times\Delta y\times\Delta z = 1.5$ fm $\times 1.5$ fm $\times 1$ fm,

$$\langle n_b\rangle = \sum_{\rm cells} n_{\rm cell}\mathsf{N}_b^{\rm cell} \Big/ \sum_{\rm cells} \mathsf{N}_b^{\rm cell} \qquad (1)$$

within a total volume of $L_x \times L_y \times L_z = 22.5\times 22.5\times 30$ fm^3. Statistics of 50 events were used for all impact parameters. The time was measured in the center-of-mass of the colliding nuclei.

We also calculated the average density over the center-of-mass volume and over the local rest frame volume of the cells. The sum runs over cells where one can find at least one baryon, i.e., $\mathsf{N}_b^{\rm cell} \neq 0$:

$$\langle n_b\rangle = \sum_{\rm cells} n_{\rm cell}\mathsf{V}_{\rm cell} \Big/ \sum_{\rm cells} \mathsf{V}_{\rm cell} \qquad (2)$$

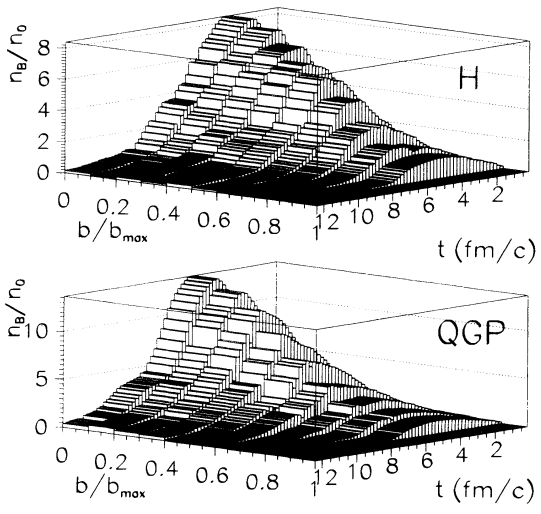

FIG. 1. Central baryon density, n_B/n_0, evaluated in a volume of 5 fm^3 as a function of time and impact parameter, $b/b_{\rm max} = 0$–1, in an Au+Au collision at 11.6A GeV/c, for a QGP (lower figure) and hadronic (upper figure) EOS calculated in the fluid dynamical model.

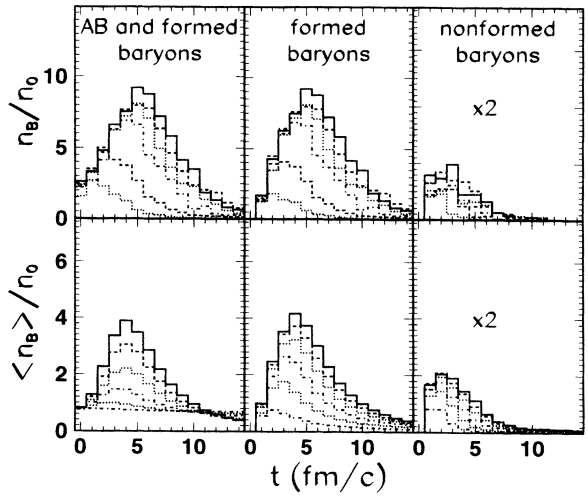

FIG. 2. Central (upper) baryon density, n_B/n_0, in a volume of 3 fm^3 and average (lower) baryon density, n_B/n_0, vs time and impact parameter, $b = 2$–4–6–8–10–12 fm, calculated in the QGSM for all baryons which passed their formation time (AB+formed) and newly formed baryons (formed) in Au+Au collisions. The contribution of the latent baryon number inside nonhadronized strings (nonformed baryons) is plotted separately. The density increase is the largest for the smallest impact parameter.

and

$$\langle n_b\rangle = \sum_{\rm cells} n_{\rm cell}\gamma_{\rm cell}\mathsf{V}_{\rm cell} \Big/ \sum_{\rm cells} \gamma_{\rm cell}\mathsf{V}_{\rm cell}. \qquad (3)$$

The difference between definitions (2) and (3) is about 15–20%, while using definition (1) obtains a result two times larger than using definition (2).

In the same manner as the baryon density we investigated the density of the mesons. In the QGSM the maximal central (average) density of all mesons, produced in the central Au+Au collisions is about 21(10) n_0 at t=5(4) fm/c, while for nonformed mesons this value is 2 times smaller, 10(5)n_0 at $t = 4$ fm/c.

In the QGSM we can trace the space-time evolution of different particle species, i.e., target and projectile baryons and mesons (AB baryons), newly formed hadrons, as well as the nonformed hadrons which are present as strings during the middle stages of the reaction until their formation time elapses (Fig. 3). The number of string hadronizations or *cascades* are also shown as well as the number of final *decays* of excited hadronic states arising from string fragmentation. The number of original nucleons from the projectile and target (AB nucleons) gradually decreases, particularly in nearly central collisions (Fig. 3).

The baryon rapidity distributions indicate strong stopping for both EOSs, but their dependence on the breakup time and on the EOS is about the same. In both cases the rapidity distribution peaks at $dN_B/dY \approx 80$ with a small dip in the middle (Fig. 4). Thus, the baryon rapidity distribution is not an obvious signal for the phase transition. With a QGP, the final longitudinal extent of the rapidity

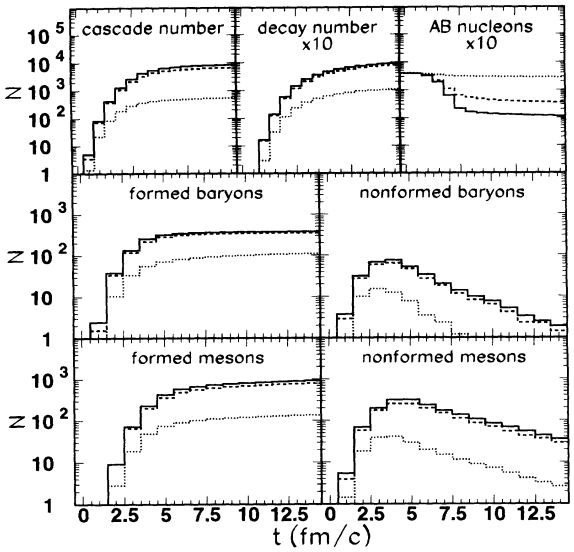

FIG. 3. Time development of the number of different hadronic species according to the QGSM for three different impact parameters, $b = 1$ fm (full curve), 3 fm (dashed), and 10 fm (dotted).

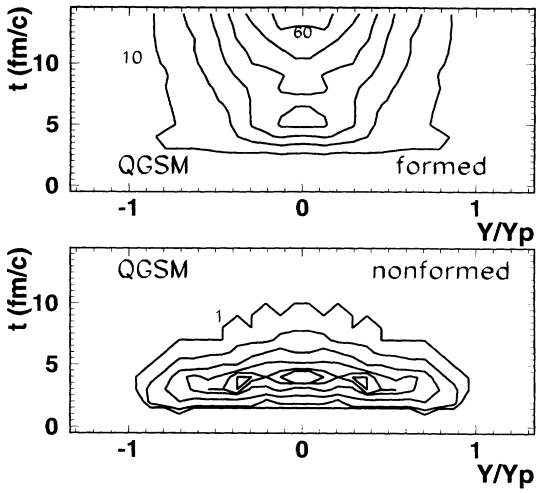

FIG. 5. Contour plots of the proton rapidity distribution calculated in the QGSM for nearly central ($b = 3$ fm) Au+Au collisions at 11.6A GeV/c as a function of time for formed (upper plot) (dN/dY = 10, 20, 30, 40, 50, and 60) and for nonformed protons (lower) (dN/dY = 1, 2.5, 5, 7.5, and 9) inside nonhadronized strings.

distribution is larger (see Fig. 4). This enhanced longitudinal motion is a clear consequence of the fact that at the stage of maximum compression, the matter described by the QGP EOS is more compressed, which results in a more elongated shape for the compressed matter; consequently, the pressure gradients initially accelerate the system longitudinally, while the transverse expansion is reduced. We can also observe that while the increase of longitudinal motion is smooth and gradual in the case of hadronic matter (Fig. 5, upper), for the QGP the expansion is initially slow and it suddenly becomes rapid when the hadronization is completed and the matter is in the pure hadronic phase, around $t = 6 - 8$ fm/c (Fig. 5, lower). By this time in the case of the hadronic EOS the longitudinal expansion is fully saturated. The width of the proton rapidity distribution at freezeout is the same as observed experimentally [5].

In the QGSM the rapidity distributions of protons and negatives indicate similarly strong stopping [5] and the rapidity distribution peaks at $dN_B/dY \approx 80$, in good agreement with experimental data [8]. The spectra are even more peaked than in the fluid dynamical model (see

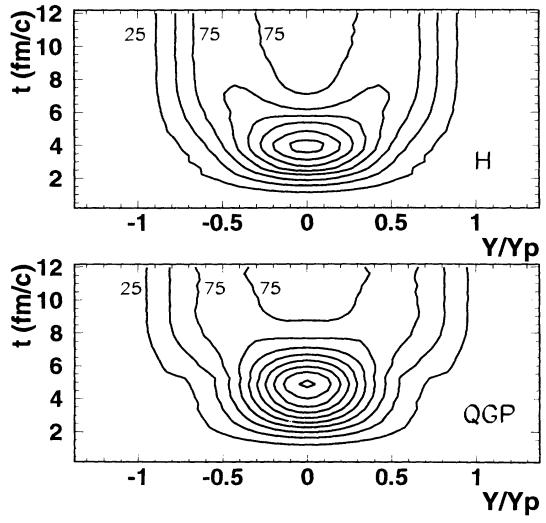

FIG. 4. Contour plots of the proton rapidity distribution calculated in the fluid dynamical model for nearly central ($b/b_{max} = 0.2$) Au+Au collisions at 11.6A GeV/c as a function of time for a hadronic (upper) and a QGP (lower) EOS. The increment between two neighboring contour lines is $\Delta(dN_B/dY) = 25$.

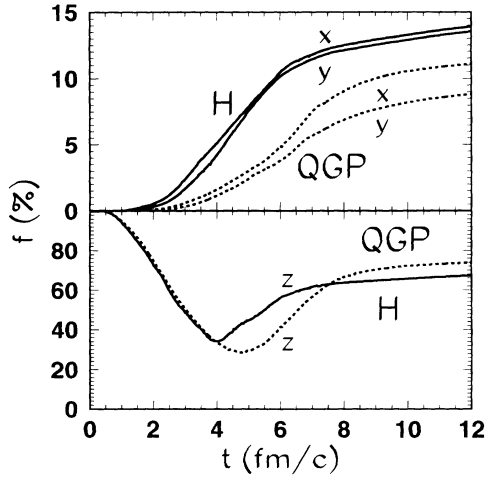

FIG. 6. Diagonal elements of the momentum flow tensor, $F_j = \sum_{\text{cells}} p_j p_j$, in the direction of reaction plane (x) and in the squeeze-out direction (y) as a function of time. The quantity is normalized to the initial value of the longitudinal component: $f_j \equiv F_j/F_z(t = 0)$, for a nearly central ($b/b_{max} = 0.2$) Au+Au collision at 11.6A GeV/c for hadronic (full curves) and QGP (dashed curves) EOSs.

Fig. 4). The rapidity distribution of nonformed baryons (nonhadronized strings) may be considered as a precursor to a QGP or to a mixed phase. Its time extent is short, 3–4 fm/c only, but its extent in rapidity is much wider than the width of the rapidity distribution of the dense region in the fluid dynamical model with a QGP EOS (Fig. 5). The target and projectile spectators (not shown) maintain their rapidities; however, their abundance decreases rapidly and it reaches one-tenth of the original volume by t =7 fm/c.

III. COLLECTIVE FLOW IN TRANSVERSE DIRECTIONS

In the fluid dynamical model the average transverse momentum for baryons, $< p_t/A >$, is about 1.3 GeV/c at all rapidities. It does not depend strongly on the EOS, the difference being about 10%. The pion $p_\perp$ and rapidity distribution are even less of a phase transition signal, because in the fluid dynamical model we consider thermal pions at their breakup only. The final pion distribution depends very strongly on the selected breakup time. This is because of the extremely strong temperature dependence of the multiplicity and of the thermal pion spectra. In the QGSM the average transverse flow for baryons does not have a strong rapidity dependence either, but it is much smaller than in the fluid dynamical model (about 0.5 GeV/c). The difference between the fluid dynamical model and QGSM predictions of $\langle p_t/A \rangle$ (as well as $\langle p_x/A \rangle$) can arise for many reasons, one of which is the absence of viscosity in the fluid dynamical model.

A. Momentum flow tensor

It should not surprise us that the collective fluid dynamical effects are exhibited much more clearly at small impact parameters than for peripheral reactions. We have studied the Au+Au reaction at $b/b_{\max} = 0.2$. We can characterize the collective flow in the $j = x$ (transverse direction in the reaction plane), y (out of plane), and z (beam) directions by $F_j = \sum_{\text{cells}} p_j p_j$.

In the direction of the reaction plane the diagonal element of the momentum flow tensor, F_x, is about 25% larger for the hadronic EOS at its maximum than for the QGP EOS (see Fig. 6). The strongest and most clearly observable sign of the different EOS can be seen in the squeezeout (y-) direction where the flow F_y is more than 50% larger for the hadronic EOS than for QGP EOS. As shown in Fig. 6 it is most illustrative to present the components of the momentum flow tensor, F_j, in relation to the precollision value of the longitudinal flow, i.e., $f_j = F_j/F_z(t = 0)$. For the hadronic EOS there is no essential difference between F_x and F_y, while for a QGP the difference is quite substantial. The saturation of the transverse expansion is also observably delayed compared to the longitudinal direction, and the delay is the largest in the squeezeout direction.

The longitudinal flow initially decreases strongly; in central collisions at the maximum compression it is only about 10% of the initial value, then it rises back to about 30–40% depending on the EOS [9]. At $b/b_{\max} = 0.2$, as shown in Fig. 8, the external regions maintain their longitudinal momentum during the whole collision, so that F_z decreases to about 30–35% of the initial value only. The pressure then reaccelerates the material in the longitudinal direction. In case of a QGP the compressed stage is much more elongated or prolate in the transverse direction, and this results in an expansion which is much more directed into the beam direction. Thus, by the time the final asymptotic value is obtained, the beam-directed component of the momentum flow tensor is almost 10% larger for a QGP than for a hadronic EOS.

In the QGSM we also evaluated the diagonal elements

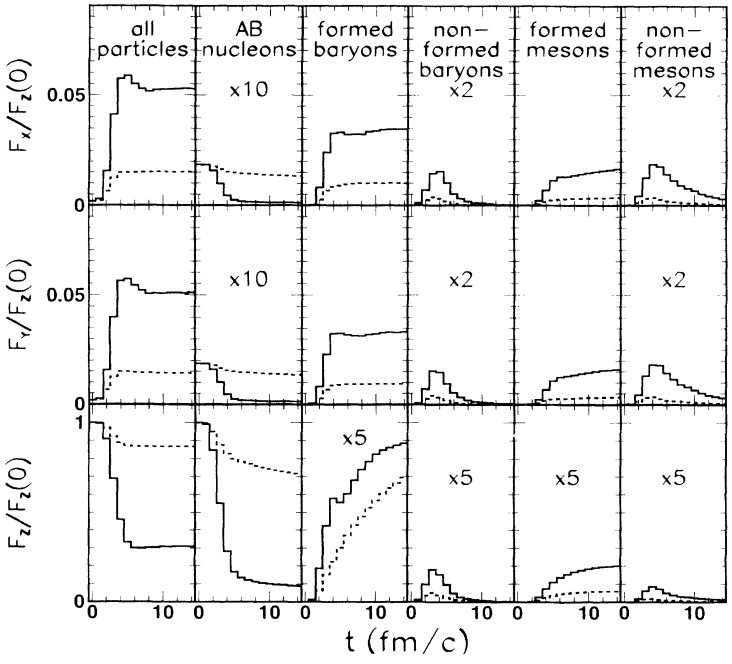

FIG. 7. Diagonal elements of the momentum flow tensor, $F_j = \sum_{\text{particles}} p_j p_j$, in the direction of the reaction plane x in the squeeze-out direction y and in the beam direction z obtained in the QGSM for all existing baryons, for nucleons of the original nuclei, formed and nonformed produced baryons and mesons. The quantity is normalized to the initial value of the longitudinal, z, component: $f_j \equiv F_j/F_z(t = 0)$, for a nearly central ($b$ = 3 fm, full curves) and a peripheral (b = 10 fm, dashed curves) Au+Au collision at 11.6A GeV/c as a function of time.

of the momentum flow tensor, $F_j = \sum_{\text{particles}} p_j p_j$, where $p_x p_x = (\mathbf{p} \cdot \mathbf{b})^2/(\mathbf{b} \cdot \mathbf{b})$, and $p_y p_y = p_t^2 - p_x^2$, for all particles, including nucleons of nuclei, formed and nonformed baryons, and mesons for central and peripheral ($b = 3$ and 10 fm) Au+Au collisions (Fig. 7). The time-development picture for F_j differs for central and peripheral collisions.

The longitudinal and transverse components of the momentum flow tensor for the original nucleons changes much slower in peripheral than in central collisions. This is connected to a tenfold increase in the number of collisions and produced particles (see Fig. 7). Baryons start to form earlier than mesons because of the large number of spectators that can interact again immediately after the primary collision. The transverse components of the momentum flow of formed baryons grow very quickly, then decrease somewhat and start to grow again around $t = 7$–8 fm/c in central collisions. This happens because of the combined effect of leading baryons formed immediately after the primary interaction and nonformed particles which carry away a part of the initial momentum during the first 2–7 fm/c, but then transfer it to the formed baryons.

In the QGSM there is no visible difference between the F_x and F_y components of momentum transverse flow for all impact parameters.

B. Transverse flow analysis

The transverse flow analysis for protons, $\langle p_x/A \rangle$, is also a sensitive indicator of the EOS according to the fluid dynamical model. The quantity $\langle p_x/A \rangle$ is much smaller than $\langle p_t/A \rangle \approx 1.3$ GeV/c. For the Au+Au, 11.6A GeV/c reaction the weighted average over impact parameters, $b/b_{\max} = 0$–0.5, $\langle p_x/A \rangle_{\max} \approx 550$ (250) MeV/c for hadronic (QGP) EOS, respectively, at the target or projectile rapidity. This impact parameter range corresponds roughly to the selection of 25% of the highest multiplicity events from the minimum bias sample (Fig. 8).

In the QGSM for Au+Au collisions the transverse flow is smaller, but remains a large and observable effect. It has a similar behavior as as in the fluid dynamical model: for protons the distribution of $\langle p_x/A \rangle$ is antisymmetric and grows smoothly from a minimum at negative rapidity values to the maximum which is about 100 MeV/c [5]. For charged particles $\langle p_x/A \rangle$ is much smaller, but also can be observed (Fig. 8). At AGS energies the azimuthal asymmetry of the emitted protons and deuterons has already been detected [10], but the transverse flow using the standard method[11] has not been evaluated yet.

C. Space-time dynamics

The space-time pattern of a collision is different in the two models, and in the fluid dynamical model it strongly depends on the EOS. Due to the higher compression with a QGP the volume of the most dense region is almost half of this volume with the hadronic EOS. On the other hand, the lifetime of the dense matter is about 60–80% longer [5, 6].

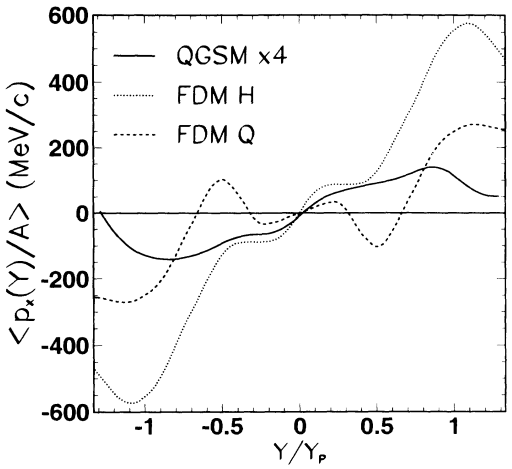

FIG. 8. Average transverse flow for protons, $\langle p_x/A \rangle$, in a Au+Au collision at 11.6 A GeV/c in the fluid dynamical model (FDM) for a QGP (dashed line) and a hadronic (H—full line) EOS plotted vs Y/Y_P. The impact parameter is averaged over $b/b_{\max} = 0$–0.5. The full line is calculated for $b = 3$ fm in the QGSM for all charged particles. In the QGSM the transverse flow for protons is 2.5 times larger Ref. [5] than for all charged particles.

In the QGSM we studied the space-time pattern of the region occupied by strings or nonformed particles. This region is wider than the dense region in fluid dynamics and it decays in a different pattern. While in fluid dynamics the dense region disappears along t=const or τ=const surfaces, in the QGSM the string-region decays at its outside surface surviving quite long in the middle, approximately 10 fm/c.

IV. SUMMARY

In conclusion, we suggest one should study the collective flow behavior in the Au+Au reactions at AGS energies. According to our theoretical predictions these collective effects are well measurable at the AGS using the same or similar methods as were used at the BEVALAC. Both the transverse flow, $\langle p_x/A \rangle$, and particularly the squeeze-out effect are particularly sensitive to the precursors of the transition to the QGP. If both the bounce-off and squeeze-out are identified the signal of the prephase transition softening of the EOS can be detected. It is indicated by the larger squeeze-out versus bounce-off ratio than measured at the BEVALAC.

A significant amount of QGP is not expected to be formed at this energy, but the signs of the phase transition due to the effects of the mixed phase are observable.

ACKNOWLEDGMENTS

This work is supported in part by the U.S. Department of Energy, by the Norwegian Research Council (NFR) under Contracts NFR-422.93/011 and NFR-422.93/007, by the NFR and the Hungarian Academy of Sciences exchange grant under Contract NFR-422.93/008, by the Hungarian Science Foundation under Grant No. OTKA-F4019, and by the NATO Scientific Affairs Division under Contract CRG.920322-644/92/JARC-501.

[1] L.P. Csernai and J.I. Kapusta, Phys. Rev. D **46**, 1379 (1992); Phys. Rev. Lett. **69**, 737 (1992).
[2] L.P. Csernai, J.I. Kapusta, Gy. Kluge, and E.E. Zabrodin, Z. Phys. C **58**, 453 (1993).
[3] N.S. Amelin *et al.*, Phys. Lett. B **261**, 352 (1991); Phys. Rev. Lett. **67**, 1523 (1991).
[4] N.S. Amelin *et al.*, Phys. Rev. C **44**, 1541 (1991).
[5] L. Bravina, N.S. Amelin, L.P. Csernai, P. Lévai, and D. Strottman, Nucl. Phys. **A566**, 461c (1994).
[6] D. Strottman, Nucl. Phys. **A566**, 245c (1994).
[7] F.H. Harlow, A.A. Amsden, and J.R. Nix, J. Comp. Phys. **20**, 119 (1976).
[8] M. Gonin *et al.*, Nucl. Phys. **A553**, 799c (1993).
[9] L. Bravina, L.P. Csernai, P. Lévai, and D. Strottman, in *Proceedings International Conference on Heavy-Ion Physics at the AGS: HIPAGS '93*, 1993 (MIT, Boston, Massachusetts), p. 329.
[10] T. Abbott *et al.*, Phys. Rev. Lett. **70**, 1393 (1993).
[11] P. Danielewicz and G. Odyniecz, Phys. Lett. **B157**, 146 (1985).